

## Epoxidized Natural Rubber Bionanocomposite: A Model Case of Bionanocomposite Using Nanofibrous Chitosan and Its Consequent Functional Properties

Tipparat Lertwattanaseri,<sup>1,4</sup> Naoya Ichikawa,<sup>2</sup> Tetuo Mizoguchi,<sup>2</sup>  
Yasuyuki Tanaka,<sup>3</sup> and Suwabun Chirachanchai<sup>\*1,4</sup>

<sup>1</sup>The Petroleum and Petrochemical College, Chulalongkorn University,  
Soi Chula 12, Phayathai Rd., Bangkok 10330, Thailand

<sup>2</sup>SRI Research & Development Ltd. (SRI R&D), Kobe 651-0071

<sup>3</sup>Faculty of Science, Mahidol University, Nakornpatom 73170, Thailand

<sup>4</sup>Center for Petroleum, Petrochemical, and Advanced Materials, Chulalongkorn University,  
Bangkok 10330, Thailand

(Received May 12, 2009; CL-090458; E-mail: csuwabun@chula.ac.th)

A bionanocomposite of epoxidized natural rubber (ENR) with nanofibrous chitosan is proposed. The bionanocomposite is formed under the reaction between epoxy groups of ENR and amino and hydroxy groups of chitosan as confirmed by qualitative and quantitative FTIR techniques. The nanofibrous chitosan induces stiffness at nanoscale as observed by AFM and tensile strength at microscale to the ENR–chitosan nanocomposite system. The nanocomposite also shows the copper ion absorptivity as investigated by SEM metal ion mapping mode.

Chitosan (Figure 1a) is the second most naturally abundant polysaccharide with wide range applications based on biorelated specific properties, metal ion chelation and absorptivity (e.g.  $\text{Cu}^{2+}$ ,  $\text{Cd}^{2+}$ , and  $\text{Ni}^{2+}$ ),<sup>1,2</sup> including the possibility of derivatization. This polysaccharide was reported for its various morphologies such as fibers,<sup>3</sup> whiskers,<sup>4–6</sup> and nanoparticles.<sup>7</sup> In the past, natural rubber nanocomposite with nano-whiskered chitin showing an improvement in mechanical properties was reported.<sup>4</sup> We found that by simply reprecipitating chitosan acetic acid solution in basic solvent under dilute conditions, nanonetwork fibrous chitosan having diameter in the range of 30–70 nm could be easily obtained as confirmed by TEM (Figure 1b).

Although rubbers are known as thermal and electrical insulator materials, an addition of conductive fillers, such as metal particles, carbon black, and graphite powder,<sup>8</sup> enables rubber composites with electrical conductivity for specific applications such as gaskets, keypads, and sensing devices.<sup>9</sup> Epoxidized natural rubber (ENR) (Figure 1c) has a reactive epoxy group to possibly form covalent bonds with chitosan (Figure 1d). The present work, thus, focuses on a bionanocomposite system of nanofi-

brous chitosan and ENR matrices. The fact that (i) chitosan is a light weight material as compared to the traditional fillers mentioned above and (ii) chitosan chelates with various metal ions, the success of ENR–nanofibrous chitosan bionanocomposite might lead to novel functional ENR products.

ENR latex was mixed with nanofibrous chitosan (%DD  $\approx$  90)<sup>10</sup> at 2.5, 5, 10, and 20 phr. Each mixture was cast on a plastic mold and dried in an oven at 60 °C to obtain dry sheets before blending with 3, 1.5, 1, and 2 phr of zinc oxide (ZnO), sulfur (S), *N*-cyclohexyl-2-benzothiazolesulfenamide (CBS), and stearic acid, using a Labtech two roll mill at 40 °C. The ENR and ENR–chitosan nanocomposites were vulcanized by a Vantage compression molding at 150 °C for the optimum cure time ( $t_{90}$ ) as determined by a Rheotch MD+ moving die rheometer (MDR).

In order to identify the structure as shown in Figure 1d, qualitative and quantitative FTIR analyses were carried out.<sup>11</sup> Figure 2A shows an example of ENR–nanofibrous chitosan bionanocomposite as compared to those of ENR and chitosan. The curve fittings in the range of 3000–2700  $\text{cm}^{-1}$  for methyl group in ENR ( $\text{CH}_3$  stretching) and of 920–770  $\text{cm}^{-1}$  for epoxy group ( $\text{C}-\text{O}-\text{C}$  bending) were done to trace how epoxy groups changed (Figure 2B). The quantitative analysis of epoxy groups based on  $\nu_{\text{as}}$  and  $\nu_{\text{s}}$  of the  $\text{CH}_3$  groups at 2960 and 2925  $\text{cm}^{-1}$  (Figure 2C) shows the amount of epoxy groups is reduced significantly in the blend with chitosan content 2.5 phr and continuously decreases for chitosan content from 5 to 20 phr. This implies a reactive blending of ENR–nanofibrous chitosan during bio-nanocomposite formation.

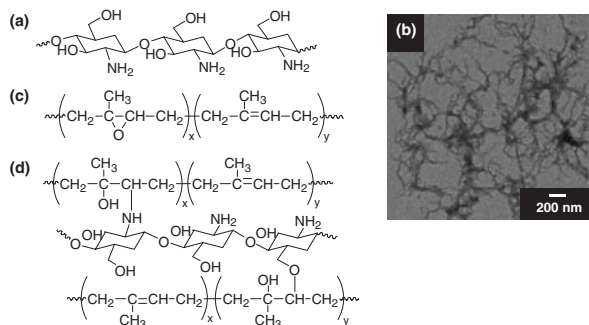


**Figure 1.** Chemical structures of (a) chitosan, and (c) ENR, (d) possible ENR–nanofibrous chitosan bionanocomposite structure, and (b) TEM micrograph of reprecipitated showing nanofibrous form.

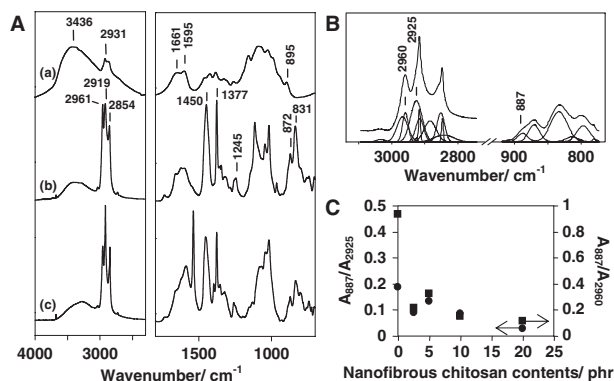


**Figure 2.** (A) FTIR spectra of (a) nanofibrous chitosan, (b) ENR, and (c) ENR–nanofibrous chitosan bionanocomposite (10 phr), (B) curve fitting of ENR–nanofibrous chitosan bionanocomposite (10 phr), and (C) quantitative analysis based on (B) at various chitosan contents.

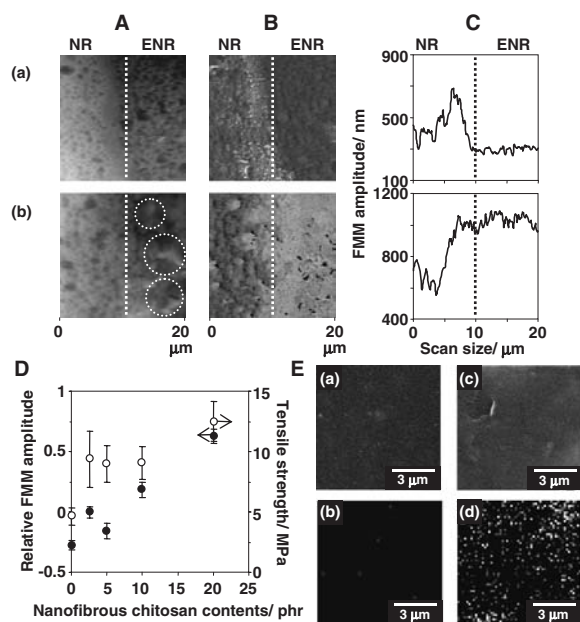


**Figure 3.** (A) Topographic AFM images, (B) FMM amplitude AFM images ( $20\mu\text{m}^2$ ), and (C) FMM amplitude profiles of: (a) ENR and (b) ENR–nanofibrous chitosan bionanocomposite ( $20\text{phr}$ ), (D) relative FMM amplitude (●) and tensile strength (○) of ENR–nanofibrous chitosan bionanocomposite with various chitosan contents, and (E) FE-SEM micrographs of: (a) surface and (b) mapping mode after immersing in copper sulfate solution of ENR, (c) surface and (b) mapping mode after immersing in copper sulfate solution of ENR–nanofibrous chitosan bionanocomposite ( $20\text{phr}$ ) (Note: For (A), (B), and (C), a reference NR was shown in the left area).

In order to evaluate the effect of nanofibrous chitosan on the surface properties of ENR, NR latex was used as a reference by coating NR on both ENR and ENR–nanofibrous chitosan bionanocomposites sample surfaces. Figure 3A shows topographic atomic force microscopy (AFM) images. As compared to the pure ENR, ENR–nanofibrous chitosan bionanocomposite displays a rough surface. This implies the existence of nanofibrous chitosan on the surface and the consequent roughness (the circular area in Figure 3Ab). Figures 3B and 3C are the FMM (force modulation microscopy) amplitude images and profiles. The pure ENR surface shows the dark area (Figure 3Ba) with a low signal in amplitude profile (Figure 3Ca). By comparing these results with those of NR reference, it is clear that the ENR surface is softer than that of NR. However, ENR–nanofibrous chitosan bionanocomposite displays a light image (Figure 3Bb) and a high amplitude profile signal (Figure 3Cb) as compared to ENR. This implies that the nanofibrous chitosan initiates stiffness onto the ENR surface. Bar et al. demonstrated a similar FMM result for alkanethiols<sup>12</sup> to conclude the stiffness of the material. The relative FMM amplitudes were evaluated using NR as a reference and were plotted against nanofibrous chitosan contents to evaluate the changes of the surface stiffness of the ENR–nanofibrous chitosan bionanocomposite (Figure 3D). The FMM amplitude increases almost linearly with an increase of nanofibrous chitosan contents which confirms the surface stiffness enhanced after adding nanofibrous chitosan.

The pure ENR (Figure 3Ea) shows a smooth surface where-as the ENR–nanofibrous chitosan bionanocomposite is rough

(Figure 3Ec) as observed by field emission scanning electron microscopy (FE-SEM), which is relevant to the topographic AFM image (Figure 3Ab). This confirms that the nanofibrous chitosan induces the rough surface to ENR. Considering the specific properties of chitosan related to the metal chelation, an immersion of ENR and ENR–nanofibrous chitosan bionanocomposite in a metal ion solution overnight was carried out. Figure 3Ed displays the surfaces of ENR–nanofibrous chitosan bionanocomposite after immersing in copper sulfate solution (2%, w/v) using copper ion FE-SEM mapping mode as compared to the pure ENR surface (Figure 3Eb). The result clearly shows the copper distribution on the bionanocomposite surface. This reflects the function of amino groups in copper absorption.<sup>1,2</sup>

It comes to the question of how those nanoscale and micro-scale structures induce changes on a millimeter scale. The ENR and ENR–nanofibrous chitosan bionanocomposite were compressed in a sheet form to evaluate the tensile strength. Figure 3D shows the plot of ENR with various nanofibrous chitosan contents to find that the tensile strength increases with an increase of chitosan content. With only 5 phr content of nanofibrous chitosan, the tensile strength is significantly increased by two times. The result is relevant to the surface stiffness in nanoscale as plotted by relative FMM amplitude.

The epoxy group of ENR allowed a reactive blend in the obtained ENR–nanofibrous chitosan bionanocomposites. The nanocomposites showed an enhancement in surface roughness and stiffness, an increase in tensile strength, and metal ion absorptivity, therefore; this bionanocomposite can be expected to be a novel ENR functional material.

The present work was supported by SRI R&D Ltd., Japan. The authors acknowledge Seafresh Chitosan (Lab) Company Limited (Thailand), Sumirubber Malaysia SDN (Malaysia), R&D Center for Thai Rubber Industry (Thailand), Labtech Company Limited (Thailand), and the Hitachi High-Technologies Corporation (Japan).

#### References and Notes

- 1 K. Kurita, T. Sannan, Y. Iwakura, *J. Appl. Polym. Sci.* **1979**, 23, 511.
- 2 F.-C. Wu, R.-L. Tseng, R.-S. Juang, *Ind. Eng. Chem. Res.* **1999**, 38, 270.
- 3 S. Hirano, K. Nagamura, M. Zhang, S. K. Kim, B. G. Chung, M. Yoshikawa, T. Midorikawa, *Carbohydr. Polym.* **1999**, 38, 293.
- 4 a) K. G. Nair, A. Dufresne, *Biomacromol.* **2003**, 4, 657. b) K. G. Nair, A. Dufresne, *Biomacromol.* **2003**, 4, 666.
- 5 S. Phongying, S.-I. Aiba, S. Chirachanchai, *Polymer* **2007**, 48, 393.
- 6 T. Lertwattanaseri, N. Ichikawa, T. Mizoguchi, Y. Tanaka, S. Chirachanchai, *Carbohydr. Res.* **2009**, 344, 331.
- 7 R. Yoksan, M. Akashi, K. Hiwatari, S. Chirachanchai, *Biopolymers* **2003**, 69, 386.
- 8 D.-Y. Jeong, J. Ryu, Y.-S. Lim, S. Dong, D.-S. Park, *Sens. Actuators, A* **2009**, 149, 246.
- 9 A. M. Shanmugharaj, J. H. Bae, K. Y. Lee, W. H. Noh, S. H. Lee, S. H. Ryu, *Compos. Sci. Technol.* **2007**, 67, 1813.
- 10 Degree of deacetylation (%) =  $\{1 - [(I_{\text{H-Ac}}/3)/(I_{\text{H-2}})]\} \times 100 = \{1 - [(0.2151/3)/(0.6877)]\} \times 100 = 89.57\%$ .
- 11 Chitosan, FTIR ( $\text{cm}^{-1}$ ): 3500–3300 (OH), 3000–2800 (C–H stretching), 1661 (amide I), and 1595 (–NH<sub>2</sub>); ENR, FTIR ( $\text{cm}^{-1}$ ): 2961, 2919, and 2854 (C–H stretching), 1450 (C–H bending of –CH<sub>2</sub>–), 1377 (C–H bending of –CH<sub>3</sub>), 870 (C–O–C bending of epoxy group), and 836 (C–H bending of C=C–H).
- 12 G. Bar, S. Rubin, A. N. Parikh, B. I. Swanson, T. A. Zawodzinski, *Langmuir* **1997**, 13, 373.